

Electronic Supplementary Information (ESI) for Chem. Comm.

Two-dimensional Core@Shell Metal–Organic Framework and Its Derived Co/Ni-Embedded N-doped Porous Carbon for Electrocatalytic Oxygen Reduction

Yang Xu,^{†, a} Zhehao Huang,^{†, b} Bin Wang,^a Chaochao Zhang,^a Zuozhong Liang,^a Yanzhi Wang,^a Wei Zhang,^a Haoquan Zheng,^{*a} and Rui Cao^{*a}

^aSchool of Chemistry and Chemical Engineering, Shaanxi Normal University, Xi'an, 710119, China.

^bDepartment of Materials and Environmental Chemistry, Stockholm University, SE-10691 Stockholm, Sweden.

Correspondence Email: zhenghaoquan@snnu.edu.cn; ruicao@ruc.edu.cn

1. Experimental section

1.1 Materials

NiCl₂·6H₂O (AR, 98%)·Co(NO₃)₂·6H₂O (99.99%), 2-Methylimidazole (98%), and Terephthalic acid (99%) were purchased from the Energy Chemical. Zn(NO₃)₂·6H₂O (99%), N, N-dimethylformamide (DMF) (99.5%) and KOH (98%) were purchased from Sinopharm Group Chemical Reagent Co., Ltd.. Methanol (AR, 99.5%) and Ethanol (AR, 99.7%) were purchased from the Tianjin Fuyu Fine Chemical Co., Ltd.. CoCl₂·6H₂O (AR, 99%) was purchased from General Reagent. All chemicals were used without further purification.

1.2 Preparation of NiCo-MOF nanosheets Materials

According to the literature report, First, DMF (32 mL), ethanol (2 mL) and water (2 mL) were mixed in a 100 mL beaker. Next, 0.75 mmol BDC was dissolved into the mixed solution under ultrasonication. Subsequently, 0.375 mmol CoCl₂·6H₂O and 0.375 mmol NiCl₂·6H₂O were added. After Co²⁺ and Ni²⁺ salts were dissolved, 8 mL TEA was quickly injected into the solution. Then, the solution was stirred for 5 min to obtain a uniform colloidal suspension. Afterwards, the colloidal solution was continuously ultrasonicated for 8 h (99 kHz) under airtight conditions. Finally, the products were obtained via centrifugation, washed with ethanol (3~5 times), and dried at room temperature.

1.3 Synthesis of two-dimensional NiCo-MOF@ZIF-L(Zn)

16 mmol 2-methylimidazole (1.3136 g) was separately dissolved in 40 mL DI water and stirred for 5 min. Next, 5 mg of the synthetic NiCo-MOF nanosheets was added and sonicated several minutes, to form A solution. Then, 2 mmol Zn(NO₃)₂·6H₂O was separately dissolved in 40 mL water, to form solution B. In the case of continuous agitation of A solution, B solution was quickly poured in, and the mixed solution was stirred at room temperature for 3 h. The obtained light purple precipitates were collected by centrifugation (6000 rpm, 5 min), washed with DI water for 3-5 times, and dried in vacuum freeze dryer for further application. In addition, as a contrast sample, ZIF-L(Zn) was prepared.

1.4 Synthesis of three-dimensional precursor NiCo-MOF@ZIF-L(Zn)@ZIF-67

First, 1 mmol Co(NO₃)₂·6H₂O was separately dissolved in 10 mL methanol, and then 0.5 g NiCo-MOF@ZIF-L(Zn) composite nanomaterials was added in this solution, to form A solution. Next, 8 mmol 2-methylimidazole (0.66 g) was separately dissolved in 10 mL methanol, to form solution B. Finally, mix the two solutions and stir at room temperature for 24 h. The obtained light purple precipitates were collected by centrifugation (6000 rpm, 5 min), washed with methanol for 3-5 times, and dried in vacuum freeze dryer for further application.

1.5 Synthesis of NiCo-NC

The 200 mg precursor NiCo-MOF@ZIF-L(Zn)@ZIF-67 powder was weighed in

a quartz boat and carbonized in a tubular furnace. Ar flow was introduced into the furnace. The air in the furnace was exhausted at the initial 40 minutes without heating, then heated to 900 °C at the heating rate of 5 °C·min⁻¹. After calcination for 2 h, the temperature was reduced to room temperature at the cooling rate of 5 °C·min⁻¹. Finally, containing Ni and Co bimetal nitrogen-doped carbon nanomaterials (NiCo-NC) were obtained.

In addition, all comparative samples, such as NC-1, NC-2, and NC-3 were pyrolyzed in the same way. (900 °C, 5 °C·min⁻¹, 2 h) to carbonization their corresponding precursor materials NiCo-MOF nanosheets, NiCo-MOF@ZIF-L(Zn) and ZIF-L(Zn) composite nanomaterial.

1.6 Characterization

Powder X-ray diffraction (PXRD) patterns of as-prepared materials were measured with a X-ray diffractometer (Bruker, D8 Advance, Cu K α , $\lambda = 1.5406 \text{ \AA}$, 40 kV/40mA). The morphology of the as-prepared material was observed with scanning electron microscopy (SEM, Hitachi, SU8020) and transmission electron microscopy (TEM, JEOL, JEM-2100). The Brunauer-Emmett-Teller (BET) specific surface area was measured in Micromeritics ASAP 2020. The X-ray photoelectron spectroscopy (XPS) analysis of the prepared materials was performed with a Kratos AXIS ULTRA XPS. Thermogravimetric analysis (TGA) was applied by heating the as-prepared sample at a rate of 10 °C min⁻¹ with N₂ and air from 20 °C to 1000 °C in a TA Instruments SDT Q600. Elemental analyzer (Vario EL III, Elementar Analysensysteme GmbH) was applied to measure the content of C, H, and N.

1.7 Electrochemical measurement

All electrochemical experiments of ORR performance were carried out on a CHI 760E Electrochemical Analyzer (CH Instruments) and a Pine Modulated Speed Rotator (Pine Research Instrumentation, Inc.) at ambient temperature. Usually, in a three-electrode configuration, all electrochemical measurements were carried out in 0.1M KOH solution, using a rotating disk electrode (RDE) with an area of 0.196 cm² or a rotating ring-disk electrode (RRDE) with an area of 0.247 cm² as the working electrode, Carbon rod as the counter electrode, and an saturated Ag/AgCl as the reference electrode. All potential in the figure was converted to reversible hydrogen electrode (RHE). The conversion formula is as follows: $E (\text{vs. RHE}) = E (\text{vs. Ag/AgCl}) + 0.197 \text{ V} + 0.059 \times \text{pH}$.

The preparation method of working electrode: 4 mg catalyst was weighed and dispersed in mixed solution containing 660 μL DI water, 330 μL ethanol and 10 μL Nafion aqueous solution (5 wt%). The mixed solution was treated by ultrasound for 1 h to form a homogeneous suspension. Then 15 μL catalyst solution was taken from the pipette and uniformly dripped onto the rotating disc electrode (RDE) (catalyst loading is about 0.3 mg cm⁻²) and 20 μL catalyst solution was taken from the pipette and uniformly dripped onto the rotating ring-disk electrode (RRDE) (catalyst loading is about 0.3 mg cm⁻²). After natural drying, a homogeneous film was formed.

For electrocatalytic oxygen reduction reaction (ORR), more than 30 min of Ar or O₂ flow should be injected into the electrolyte before measurement to ensure that the

performance of electrocatalytic oxygen reduction reaction (ORR) is tested in 0.1 M KOH electrolyte saturated with O₂. Cyclic voltammetry (CV) is performed at room temperature at a scanning rate of 10 mV s⁻¹. At room temperature, linear sweep voltammetry (LSV) with rotating disc electrodes (RDE) was performed at various rotating rate from 400 to 1600 rpm at the scanning rate of 5 mV s⁻¹. The kinetic parameters were calculated by Koutecky-Levich equation.

$$\frac{1}{J} = \frac{1}{J_K} + \frac{1}{J_L} = \frac{1}{J_K} + \frac{1}{B\omega^{\frac{1}{2}}}$$

$$B = 0.2nFC_0D_0^{\frac{2}{3}}V^{-\frac{1}{6}}$$

where J is the measured current density, J_K and J_L are the kinetic and limiting current densities, ω is the angular velocity of the disk, n is the electron transfer number, F is the Faraday constant (96485 C mol⁻¹), C₀ is the bulk concentration of O₂ (1.2 × 10⁻⁶ mol cm⁻³), D₀ is the diffusion coefficient of O₂ in 0.1 M KOH (1.9 × 10⁻⁵ cm² s⁻¹), and V is the kinematic viscosity of the electrolyte (0.01 cm² s⁻¹). The constant 0.2 is adopted when the rotation speed is expressed in rpm.

RRDE measurements were carried out with the rotating ring-disk electrode (RRDE) in O₂-saturated 0.1 M KOH solution at room temperature with a scan rate of 5 mV s⁻¹ and the ring-electron potential was set to 1.5 V vs. RHE. The diameter of the disk is 5.61 mm (0.247 cm²) and the area of the ring is 0.186 cm². The transfer electron number (n) and the hydrogen peroxide yield (H₂O₂%) were calculated with the following equation:

$$H_2O_2(\%) = 200 \times \frac{\frac{I_r}{N}}{I_d + \frac{I_r}{N}}$$

$$n = 4 \times \frac{I_d}{I_d + \frac{I_r}{N}}$$

Where I_d is the disk current; I_r is the ring current; N is the current collection efficiency of the Pt ring which is determined to be 0.37 from the LSV measurement in K₃Fe[CN]₆ solution).

Table S1. The NiCo-NC gives the electron transfer numbers (n)

| E/V | 0.2 | 0.3 | 0.4 | 0.5 | 0.6 | 0.7 | 0.8 |
|---------|------|------|------|------|------|------|------|
| NiCo-NC | 3.52 | 3.52 | 3.52 | 3.53 | 3.59 | 3.75 | 3.93 |
| Pt/C | 3.83 | 3.87 | 3.90 | 3.92 | 3.95 | 3.96 | 3.97 |

Table S2. Electrochemical ORR activities of catalysts in this work and other reported works.

| Catalyst | Electrolyte | $E_{1/2}$ vs RHE (mV) | Ref. |
|---------------------------------------|--------------------------------------|--------------------------|---|
| NiCo-NC | 0.1 M KOH | 866 | This work |
| Co/NC | 0.1 M KOH | 830 | Angew. Chem. Int. Ed., 2016, 55, 4087-4091. ^[1] |
| NGM-800 | 0.1 M KClO ₄ | 781 | Angew. Chem. Int. Ed., 2019, 58, 13354–13359. ^[2] |
| Co/N-C-800 | 0.5 M H ₂ SO ₄ | 863 | ChemElectroChem, 2019, 6, 2546-2552. ^[3] |
| N-HC@G-900 | 0.1 M KOH | 850 | Angew. Chem. Int. Ed., 2018, 57, 16511-16515. ^[4] |
| L-CCNTs-Co-800 | 0.1 M KOH | 840 | Angew. Chem. Int. Ed., 2018, 57, 13187-13191. ^[5] |
| ISAS-Co/HNCS | 0.5 M H ₂ SO ₄ | 773 | J. Am. Chem. Soc., 2017, 139, 17269-17272. ^[6] |
| Co@Co ₃ O ₄ /NC | 0.1 M KOH | 850 | Angew. Chem. Int. Ed., 2016, 55, 4087-4091. ^[1] |
| P-Co-NC-4 | 0.1 M KOH | 850 | Chem. Commu., 2018, 54, 7519-7522. ^[7] |
| CuCo@NC | 0.1 M KOH | 866 | Chem. Euro. J, 2019, 25, 12780-12788. ^[8] |
| Co/HNCP | 0.1 M KOH | 845 | ACS Catal. 2018, 8, 7879- 7888. ^[9] |
| Co-C ₃ N ₄ /CNT | 0.1 M KOH | 840 | J. Am. Chem. Soc. 2017, 139, 3336. ^[10] |

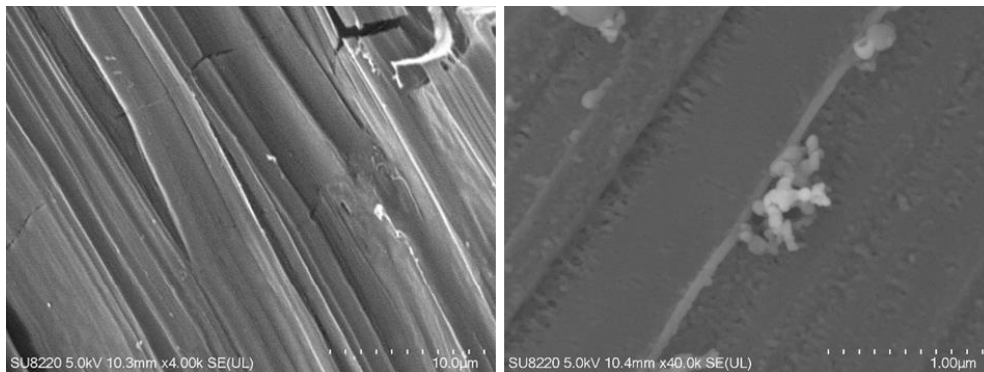


Fig. S1. SEM image of 2D NiCo-MOF after adding Hmim.

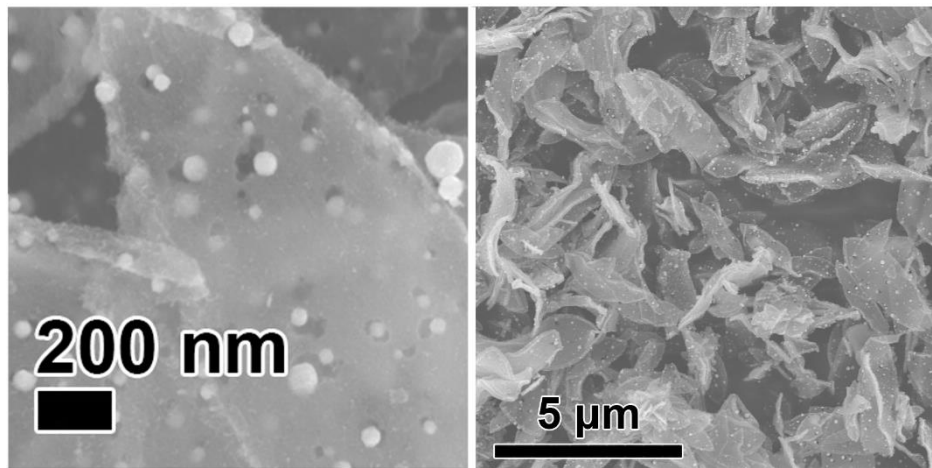


Fig. S2. SEM image of NiCo-NC.

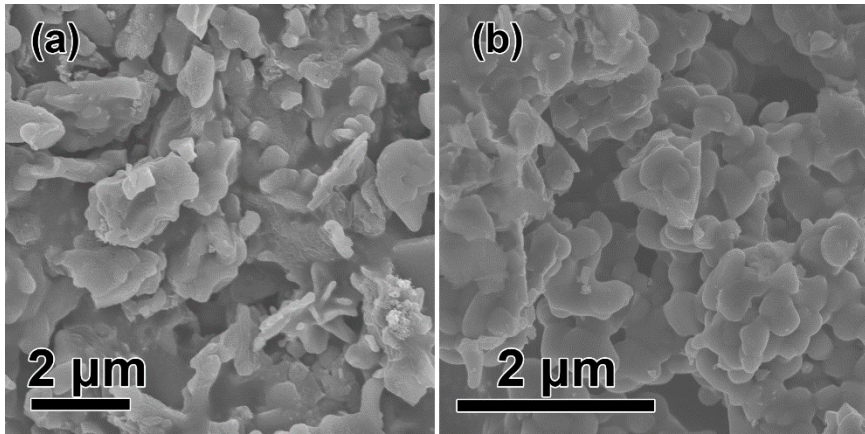


Fig. S3. SEM image of (a) NC-1 and (b) NC-2.

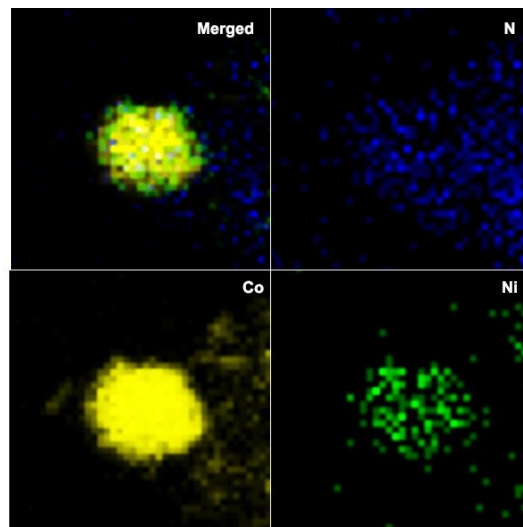


Fig. S4. EDS mapping of an individual bimetallic Ni/Co nanoparticle in NiCo-NC.

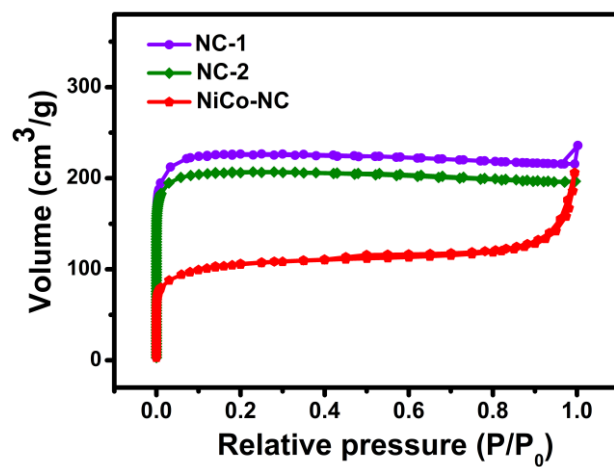


Fig. S5. N₂ adsorption-desorption isotherms of NiCo-NC.

The BET surface area of NC-1 and NC-2 is 716 m² g⁻¹ and 692 m² g⁻¹, respectively, which is higher than that of NiCo-NC. However, NC-1 and NC-2 have only small micropores and no mesopores.

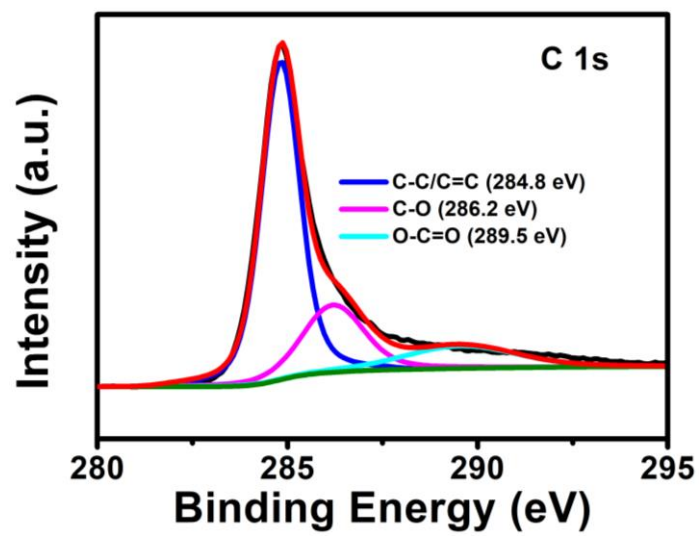


Fig. S6. XPS of C 1s of NiCo-NC.

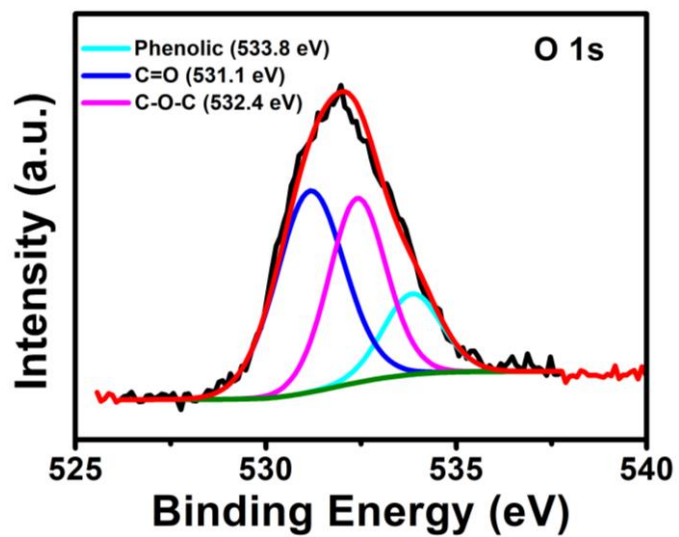


Fig. S7. XPS of O 1s of NiCo-NC.

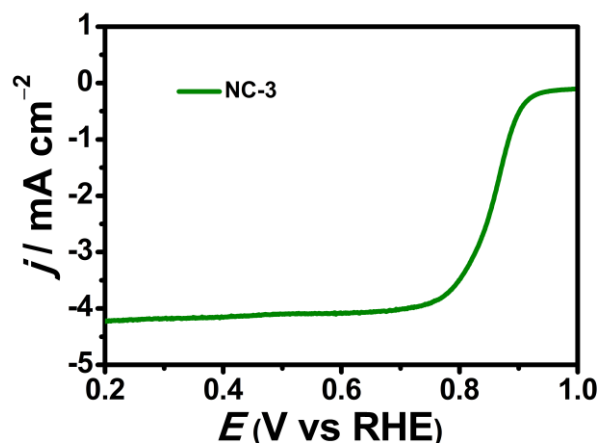


Fig. S8. LSV curves for NC-3 derived from ZIF-L(Zn)@ZIF-67 on an RDE at 1600 rpm in an O₂-saturated 0.1 M KOH.

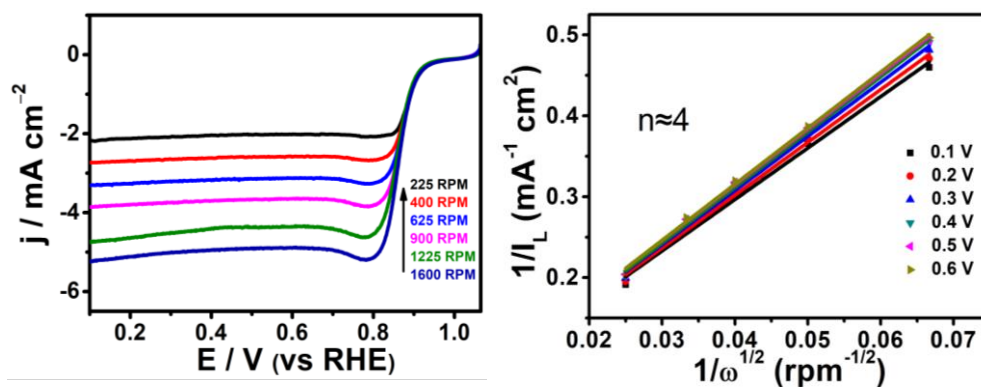


Fig. S9. RRDE measurements of LSV curves for NiCo-NC with different rotation rates in O₂-saturated 0.1 M KOH solution.

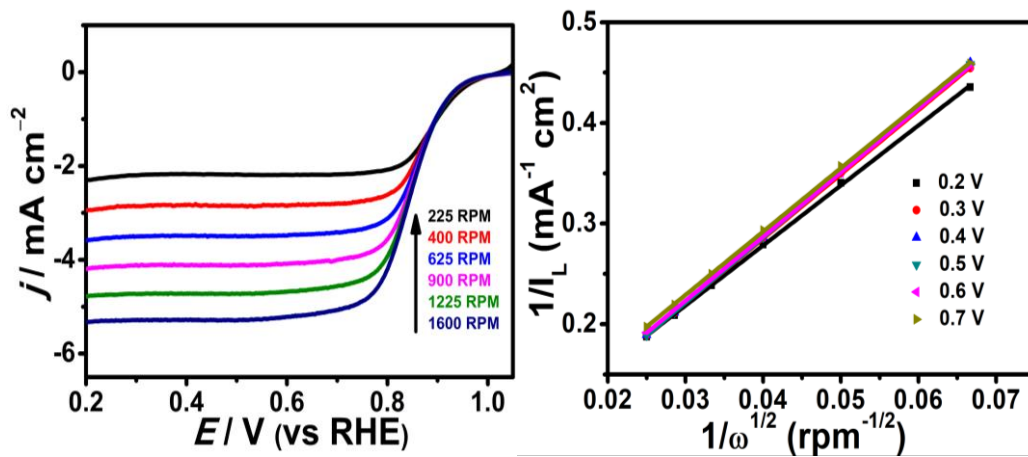


Fig. S10. RRDE measurements of LSV curves for Pt/C with different rotation rates in O₂-saturated 0.1 M KOH solution.

References:

- [1] A. Aijaz, J. Masa, C. Rösler, W. Xia, P. Weide, A. J. R. Botz, R. A. Fischer, W. Schuhmann, M. Muhler, *Angew. Chem. Int. Ed.*, **2016**, *55*, 4087-4091.
- [2] W. Xia, J. Tang, J. Li, S. Zhang, K. C. W. Wu, J. He, Y. Yamauchi, *Angew. Chem. Int. Ed.*, **2019**, *58*, 13354-13359.
- [3] Y. Bai, D. Yang, M. Yang, H. Chen, Y. Liu, H. Li, *ChemElectroChem*, **2019**, *6*, 2546-2552.
- [4] J. Sun, S. E. Lowe, L. Zhang, Y. Wang, K. Pang, Y. Wang, Y. Zhong, P. Liu, K. Zhao, Z. Tang, H. Zhao, *Angew. Chem. Int. Ed.*, **2018**, *57*, 16511-16515.
- [5] Z. Liang, X. Fan, H. Lei, J. Qi, Y. Li, J. Gao, M. Huo, H. Yuan, W. Zhang, H. Lin, H. Zheng, R. Cao, *Angew. Chem. Int. Ed.* **2018**, *57*, 13187-13191.
- [6] Y. Han, Y.-G. Wang, W. Chen, R. Xu, L. Zheng, J. Zhang, J. Luo, R.-A. Shen, Y. Zhu, W.-C. Cheong, C. Chen, Q. Peng, D. Wang, Y. Li, *J. Am. Chem. Soc.*, **2017**, *139*, 17269-17272.
- [7] Z. Liang, C. Zhang, H. Yuan, W. Zhang, H. Zheng, R. Cao, *Chem. Commun.*, **2018**, *54*, 7519-7522.
- [8] M. Huo, B. Wang, C. Zhang, S. Ding, H. Yuan, Z. Liang, J. Qi, M. Chen, Y. Xu, W. Zhang, H. Zheng, R. Cao, *Chem. Eur. J.*, **2019**, *25*, 12780-12788.
- [9] D. Ding, K. Shen, X. Chen, H. Chen, J. Chen, T. Fan, R. Wu, Y. Li, *ACS Catal.* **2018**, *8*, 7879-7888.
- [10] Y. Zheng, Y. Jiao, Y. Zhu, Q. Cai, A. Vasileff, L.-H. Li, Y. Han, Y. Chen, and S.-Z. Qiao, *J. Am. Chem. Soc.* **2017**, *139*, 3336-3339.